Actinide Neutron-Induced Fission up to 20 MeV

V.M. Maslov*

Radiation Physics and Chemistry Problems Institute, Minsk-Sosny, Belarus

Lectures given at the
Workshop on Nuclear Data and Nuclear Reactors:
Physics, Design and Safety
Trieste, 13 March - 14 April 2000

LNS015007

*maslov@sosny.bas-net.by

Abstract

Fission and total level densities modelling along with double-humped fission barrier parameters allow to describe available actinide neutron-induced fission cross section data in the incident neutron energy range of ~10 keV - 20 MeV. Saddle asymmetries relevant to shell correction model calculations influence fission barriers, extracted by cross section data analysis. The inner barrier was assumed axially symmetric in case of U, Np and Pu neutron-deficient nuclei. It is shown that observed irregularities in neutron-induced fission cross section data in the energy range of 0.5-3 MeV could be attributed to the interplay of few-quasiparticle excitations in the level density of fissioning and residual nuclei. Estimates of first-chance fission cross section and secondary neutron spectrum model were validated by ^{238}U fission, (n,2n) and (n,3n) data description up to 20 MeV.

1 Introduction

A major advance in fission reaction theory is due to the Strutinsky [1], after he discovered that the inclusion of single-particle shell corrections to a smooth liquid drop barriers leads to double-humped fission barrier for actinide nuclei. Basically, an intermediate well appeared due to shell modulation of potential energy at quadrupole deformations about three times as large as those of equilibrium ground state. The minimum excitation energy in intermediate well was predicted to be 2-3 MeV above the primary well. This picture provided an explanation for the short-lived spontaneously fissioning isomers [2], sub-barrier vibrational resonances, excited in particle transfer reactions [3], followed by fission and various resonance clustering and structures in neutron-induced reactions [4]. As a consequence of shell correction modulation of potential energy, a hierarchy of states appears. Compound states in primary well are termed a class-I states, excited compound states in intermediate well are called class-II states, pure vibrational states in the second well could be coupled with class II states. This coupling is called damping of vibrational resonances. In other words, relatively simple vibrational states could be fragmented over more complex class II compound states. The damping width is correlated with observed width of resonances in fission probability, measured with particle transfer reactions like (d,pf), (^{3}He,df), (t,pf) etc. reactions. Because of smaller damping, vibrational resonances are observed in even-even nuclides in particle transfer reactions, but rarely observed in case of odd-A and never observed in case of odd-odd nuclei. In two latter cases densities of fission transition are higher than for even-even nuclei and damping width is higher than average spacing of fission transition states. In even-even U, Pu and Cm fissioning nuclei, investigated in particle transfer reactions by [3], a number of damped vibrational resonances was observed below neutron binding energy for ^{232}U, ^{234}U, ^{236}U, ^{238}U, ^{240}U, ^{240}Pu, ^{242}Pu, ^{250}Cm and some other nuclides. That means in neutron-induced reactions on fissile nuclei, Z-even, N-odd targets none of the vibrational or class-II resonances would be observed. However some clustering of 1^+ fission resonances was attributed to class II resonance evidence in ^{239}Pu(n,f) fission reaction [5].

In case of N-odd fissioning nuclei, either Z-even or Z-odd, fission probability data [6] generally does not show any vibrational resonance structure. In case of neutron-induced fission of N-odd targets, when neutron inelastic scattering strongly competes with fission, class II resonance structures are observed for a number of target nuclides: ^{234}U, ^{238}U, ^{240}Pu, ^{242}Pu, ^{237}Np etc. because of much higher resolution in neutron-induced reactions. There are also some cases when damped vibrational resonances are evident in neutron-induced fission reactions, i.e. 0.55- and 0.78-MeV resonances in ^{234}U(n,f) data [4].

Summarizing, one would say that experimental evidences of double-humped fission barrier strongly depend on it's structure, i.e. on the relative heights of inner and outer fission barrier humps and possible split of outer fission barrier humps for Th and Pa nuclei. Here we will concentrate on the analysis of neutron-induced

fission data for actinides with Z$\geq$ 92, above $\sim$10 keV within a statistical model, disregarding structures due to class II or vibrational resonances. For non-fissile target nuclei in sub-threshold energy region we would not address the consequences of intermediate structure in fission cross sections and deal only with "gross shape" of fission cross section. However we would try to ensure that extracted fission barrier parameters are compatible with those used for analysis of neutron fission resonance clusters [7, 8].

Neutron-induced fission cross section data base for heavy actinides (U, Np, Pu, Am, Cm, Bk, Cf) provides a fair chance to develop a theoretical tools to predict competing reaction cross sections, like neutron inelastic scattering, radiative capture, (n,2n) and (n,3n) in an incident neutron energy region up to 20 MeV or higher. In most cases fission data description serves as the only constraint for these reaction cross section estimation. At the other hand, theoretical calculations are desirable to fill the gaps for nuclei where fission cross section data are lacking. For this purpose theoretical parameter systematics are highly desirable for smooth interpolations. Fission barrier parameters and fissioning nucleus level densities are key ingredients involved in neutron-induced actinide fission cross section calculations. Confidence with which theoretical fission barrier parameters could be calculated from Strutinsky-type theory [1] (Shell Correction Method (SCM)) is not better than $\sim$1 MeV, which is completely unacceptable for neutron-induced fission cross section data prediction. Anyway, theoretical fission barrier parameter trends, especially for neutron-rich nuclei, might be of some value. General trends inferred from SCM calculations [9] might be correlated with the irregularities, evident in fission cross sections data. Fission level density might be considered to be in a worse shape than level density at equilibrium deformation, since there is no relevant direct measured data. Neutron-induced fission cross section data provide a sound basis to extract fission barrier parameters, elaborate level density modelling approach [10, 11] and check it's validity up to 20 MeV [12]. Irregularities in fission cross sections in MeV incident neutron energy region would be investigated, to correlate them with theoretical fission barrier and level density parameter trends. The important point is that fission level density and barrier parameters are strongly interdependent. The level density of deformed nucleus depends on collective properties, pair correlations and shell structure of nucleus. These effects were introduced in SCM calculations of fission barriers and they should be "imbedded" into the level density model either at saddle and equilibrium deformations. These could be accomplished within framework of generalized superfluid model [13].

The impact of pair correlation, collective and shell effects on calculated fission cross sections varies with increasing excitation energy [14], [15]. There exist a lot of experimental signatures which would be used to test the validity of the model and importance of collective, pairing and shell effects at equilibrium and saddle deformations. It will be shown that observed irregularities in neutron-induced fission cross section data below $\sim$3 MeV could be attributed to the interplay of few-quasiparticle

excitations in the level density of fissioning and residual nuclei [16, 17]. At higher energies excitations shell and collective effects in level density are shown to be important for fixing fission probabilities of nuclei emerging in emissive fission reaction and contributing to total fission cross section via non-emissive fission reaction. The shell structure effects are usually introduced as level density $a-$parameter dependence on the excitation energy. The shell effects damping affects the first chance fission cross section behavior at excitation energies above emissive fission threshold. Consistent description of available fission and competing (n,2n), (n,3n) and secondary neutron spectra data for ^{238}U target nuclide would demonstrate the validity of statistical theory approach up to 20 MeV incident neutron energy.

2 Fission cross section below emissive fission threshold

Average fission cross sections are treated within Hauser-Feshbach-Moldauer theory [18, 19], coupled channel optical model and double humped fission barrier model [1]. In case of actinide fissioning compound nuclei produced by fast neutron interaction with target nuclei, the main competing channels against fission are neutron scattering and radiative neutron capture. Below there is a short outline of the statistical model employed. For even-even target nuclei we employed deformed optical potential parameters, defined by fitting total cross section data, angular distributions and $s-$wave strength function for ^{238}U [20]. For other nuclei the quadrupole β_2 and hexadecapole β_4 deformation parameter values were obtained by fitting respective $s-$wave neutron strength function $\langle S_o \rangle$ values for relevant nucleus.

The pair correlation effects in fission are well-known in case of even-even fissioning nuclei [21]. Step-like structure of the K_o^2 parameter, defining the angular anisotropy of fission fragments was interpreted to be due to few-quasiparticle excitations at saddle deformations. Few-quasiparticle effects which are due to pairing correlations are essential for state density calculation at low intrinsic excitation energies. There exist also a lot of irregularities in measured neutron-induced cross section data either for even-even, even-odd and odd-odd target nuclei. These structures are much more sensitive to the detailed fission level density shape, than K_o^2 parameter. Basically those are steps or resonance-like structures well-above fission threshold in case of $Z-$even, $N-$even targets or step-like structures in case of $Z-$even ($Z-$odd), $N-$odd targets [16, 17]. We will demonstrate below that observed irregularities in neutron-induced fission cross section data up to $\sim$3 MeV for actinide target nuclei with various parity of neutrons and protons, could be attributed to the interplay of few-quasiparticle excitations in the level density of fissioning and residual nuclei.

2.1 Statistical model

Below incident neutron energy equal to the cut-off energy of discrete level spectra the neutron cross sections were calculated within Hauser-Feshbach statistical theory approach with correction for width fluctuation [19]. Neutron-induced fission reaction cross section up to emissive fission threshold is given by

$$\sigma_{nf}(E) = \frac{\pi \lambda^{2}}{2(2I+1)} \sum_{ljJ\pi} (2J+1) T_{lj}^{J\pi}(E) P_{f}^{J\pi}(E) S_{nf}^{ljJ\pi}. \quad (1)$$

Here, the fission probability of the compound nucleus with excitation energy U for given spin J and parity π, $P_f^{J\pi}(E)$, is

$$P_{f}^{J\pi}(E) = \frac{T_{f}^{J\pi}(U)}{T_{f}^{J\pi}(U) + T_{n}^{J\pi}(U) + T_{\gamma}^{J\pi}(U)}, \quad (2)$$

where $U = B+E$ is the excitation energy of the compound nucleus, B is the neutron binding energy, E is the incident neutron energy, $T_{lj}^{J\pi}$ are the entrance neutron transmission coefficients for the channel $(ljJ\pi)$, $\vec{J} = \vec{I} + \vec{j}$, $\vec{j} = \vec{l} + \vec{s}$, I is the target nucleus spin, l an s are orbital momentum and spin of the neutron, $T_f^{J\pi}$, $T_n^{J\pi}(U)$ and $T_\gamma^{J\pi}(U)$ are the transmission coefficients of fission, neutron (elastic or inelastic) scattering and radiative decay channels, and $S_{nf}^{ljJ\pi}$ denotes partial widths Porter-Thomas fluctuation factor. For any exit channel width fluctuation factor $S_{nx}^{ljJ\pi}$ is defined as:

$$S_{nx}^{ljJ\pi} = \langle \frac{T_{nlj}^{J\pi} T_{x}^{J\pi}}{\Gamma^{J\pi}} \rangle / \frac{\langle T_{nlj}^{J\pi} \rangle \langle T_{x}^{J\pi} \rangle}{\langle T^{J\pi} \rangle} = \quad (3)$$

$$\langle T^{J\pi} \rangle \int_{0}^{\infty} \frac{(1 + 2\frac{\delta_{nx}}{\nu_{nx}})}{(1 + \frac{2}{\nu_{nlj}^{J\pi}} \langle T_{nlj}^{J\pi} \rangle t)^{1+\delta_{nx}+\nu_{nlj}^{J\pi}/2} (1 + \frac{2}{\nu_{f}^{J\pi}} \langle T_{f}^{J\pi} \rangle t)^{\delta_{fx}+\nu_{f}^{J\pi}/2}} \times$$

$$\frac{\exp(-\langle T_{\gamma}^{J\pi} \rangle t) dt}{\prod_{n'l'j'} (1 + \frac{2}{\nu_{n'l'j'}^{J\pi}} \langle T_{n'lj}^{J\pi} \rangle t)^{\delta_{n'x}+\nu_{n'l'j'}^{J\pi}/2}}$$

For width fluctuation correction calculation only Porter-Thomas fluctuations are taken into account, justification for this is provided below. Effective number of degrees of freedom for fission channel is defined at the higher fission barrier saddle as $\nu_f^{J\pi} = \mathrm{T}_f^{J\pi} / \mathrm{T}_{f\,\max}^{J\pi}$, where $\mathrm{T}_{f\,\max}^{J\pi}$ is the maximum value of the fission transmission coefficient $\mathrm{T}_f^{J\pi}$. At incident neutron energy higher than cut-off energy of discrete levels an approach by Tepel et al. [22] is employed.

2.2 Fission Channel

In a Back et al. [3] model double humped fission barrier is approximated by three parabolic sections, which are defined by six parameters: E_{fA}, $\hbar\omega_A, E_{fII}$,

$\hbar\omega_{II}, E_{fB}$, $\hbar\omega_B$, heights and curvatures of inner hump A, outer hump B and the second minimum II. Intermediate well influences on fission decay basically in two ways, i.e. fission may emerge by direct transmission of fission barrier and after absorption in the intermediate well. Relative contributions of these processes depend on the shape of fission barrier, actually on the intermediate well depth. Transmission resonances influence both transmitted and absorbed flux. Fission cross section may exhibit three kinds of structures due to: the most widely spaced vibrational resonances, class II compound states in intermediate well and most closely spaced class I compound states in the first well. Ideally, for fission data analysis in case of even-even fissioning nuclei penetrability of double-humped fission barrier should be calculated in a straightforward manner by solving Shrödinger equation. To estimate a transmission coefficient $T_f^{J\pi}$ through fission barrier one should assume that an incoming unity flux splits into three parts, a directly transmitted flux T_D, reflected flux R and absorbed flux A,while

$$T_D + A + R = 1. \tag{4}$$

An absorbed flux was introduced to interpret the increased width of sub-barrier fission resonances, observed in particle transfer fission reactions , as compared with width predictions based on resonant penetration of double humped barrier. Absorbed flux A could contribute to fission transmission coefficient $T_f^{JK\pi}\ (U)$ defined as

$$T_f^{JK\pi}(U) = T_{fD}^{JK\pi}(U) + T_{fI}^{JK\pi}(U). \tag{5}$$

Here, K is a spin $\overrightarrow{J}$ projection on the nuclear symmetry axis, quantum numbers set $JK\pi$ uniquely defines a fission channel and we will keep it where appropriate. We assume that fission barrier parameters E_{fA}, $\hbar\omega_A, E_{fII}, \hbar\omega_{II}, E_{fB}$, $\hbar\omega_B$ are independent on the fission channel parameters $JK\pi$. The first component of Eq.(5) $T_{fD}^{JK\pi}(U)$ corresponds to direct fission, while the second to that from absorbed flux in the second well:

$$T_{fI}^{JK\pi}(U) = A^{JK\pi}\frac{T_{fB}^{JK\pi}}{T_{fA}^{JK\pi} + T_{fB}^{JK\pi}}. \tag{6}$$

One of the central assumptions of the double humped fission barrier model is the so-called $K-$mixing in the second well upon absorption:

$$T_{fI}^{JK\pi}(U) = (\sum_{K=-J}^{J} A^{JK\pi})\frac{T_{fB}^{JK\pi}}{\sum\limits_{K=-J}^{J} T_{fA}^{JK\pi} + \sum\limits_{K}^{J} T_{fB}^{JK\pi}} \tag{7}$$

That means any K component could make a contribution to fission transmission coefficient $T_{fI}^{JK\pi}(U)$, gamma-decay in intermediate well being disregarded. Fission transmission coefficient $T_f^{J\pi}(U)$ is defined as a sum of $T_f^{JK\pi}(U)$ over K :

$$T_f^{J\pi}(U) = \sum_{K=-J}^{J} (T_{fD}^{JK\pi}(U) + T_{fI}^{JK\pi}(U)) =$$

$$\sum_{K=-J}^{J} \left[T_{fD}^{JK\pi}(U) + N_{abs}^{J\pi}(U) \frac{T_{fB}^{JK\pi}(U)}{\sum\limits_{K=-J}^{J} T_{fA}^{JK\pi}(U) + \sum\limits_{K}^{J} T_{fB}^{JK\pi}(U)} \right]$$

$$= \left[T_D^{J\pi}(U) + N_{abs}^{J\pi}(U) \frac{T_{fB}^{J\pi}(U)}{T_{fA}^{J\pi}(U) + T_{fB}^{J\pi}(U)} \right], \tag{8}$$

$$N_{abs}^{J\pi}(U) = (\sum_{K=-J}^{J} A^{JK\pi}) \tag{9}$$

Direct fission transmission coefficient $T_{fD}^{J\pi}(U)$ is defined as a penetrability through the double-humped fission barrier: $T_{fD}^{JK\pi}(U) = P_{fAB}^{JK\pi}(U)$. Previous equations for $T_f^{J\pi}(U)$ correspond to one class II level situation, averaged over D_{II}. For many-level of class II situation indirect fission transmission coefficient $T_{fI}^{J\pi}(U)$ could be defined [23] with weighting function $f(U - \overline{U}, W, D_{II}) = f(U - \overline{U})$, $\overline{U}$ being the excitation energy of class II state, as

$$T_{fI}^{JK\pi}(U) = \frac{N_{abs}^{J\pi}(U) T_{fB}^{JK\pi}(U)}{(T_{fA}^{JK\pi}(U) + T_{fB}^{JK\pi}(U))} f(U - \overline{U}). \tag{10}$$

Weighting function $f(U - \overline{U}, W, D_{II})$ depends on excitation energy U, width of class II states

$$W^{J\pi} = \frac{D_{II}^{J\pi}}{2\pi} \frac{1}{2} (T_{fA}^{J\pi}(U) + T_{fB}^{J\pi}(U))$$

and their spacing D_{II}. For uniform class II levels it is defined by adding Lorentzian tails from all the class II states [23]:

$$f(U - \overline{U}, W, D_{II}) = \frac{D_{II}^{J\pi}}{\pi} \sum_{n=-\infty}^{\infty} \frac{1}{(nD_{II} - (U - \overline{U}))^2 + W^2} \tag{11}$$

For equidistant class II resonances with constant width $W^{J\pi}$ one gets

$$f(U - \overline{U}) = \frac{\sinh\left(\frac{2\pi W^{J\pi}}{D_{II}^{J\pi}}\right)}{\cosh\left(\frac{2\pi W^{J\pi}}{D_{II}^{J\pi}}\right) - \cos\left(\frac{2\pi (U - \overline{U})}{D_{II}^{J\pi}}\right)} \tag{12}$$

When $W \gg D_{II}$ and in case of complete damping, $f(U - \overline{U})$ diminishes, while $T_D^{J\pi}(U)$ reaches zero, then $N_{abs}^{J\pi}(U) = T_{fA}^{J\pi}(U)$, and we get the simplest expression

for fission transmission coefficient:

$$T_f^{J\pi}(U) = \frac{T_{fA}^{J\pi}(U) T_{fB}^{J\pi}(U)}{T_{fA}^{J\pi}(U) + T_{fB}^{J\pi}(U)}. \tag{13}$$

That is a strong coupling expression for transmission coefficient of double-humped fission barrier. Analyzing neutron-induced fission data in a double humped fission barrier model, fission process can be viewed as a two-step process, i.e. a successive crossing over the inner hump A and over the outer hump B. For fission width usual expression holds:

$$\Gamma_f^{J\pi}(U) = \frac{D^{J\pi}}{2\pi} T_f^{J\pi}(U). \tag{14}$$

The penetration factors of $T_{fi}^{JK\pi}(i = A, B)$ are defined by Hill-Wheeler formula, which defines a transmission factor of parabolic barrier:

$$T_{fi}^{JK\pi}(U) = \frac{1}{(1 + \exp(\frac{2\pi}{\hbar\omega_i}(E_{fi} + \varepsilon_{fi}^{JK\pi} - U))}, \tag{15}$$

here $\varepsilon_{fi}^{JK\pi}$ are transition states at saddle point deformations. At higher excitation energies transmission coefficient $T_{fi}^{J\pi}(U)$ for the fission barrier hump is defined by the level density $\rho_{fi}(\epsilon, J, \pi)$ of the fissioning nucleus at the inner and outer humps ($i = A, B$, respectively):

$$T_{fi}^{J\pi}(U) = \sum_{K=-J}^{J} T_{fi}^{JK\pi}(U) + \int_0^U \frac{\rho_{fi}(\epsilon, J, \pi) d\epsilon}{(1 + \exp(2\pi(E_{fi} + \epsilon - U)/h\omega_i))}, \tag{16}$$

where the first term denotes the contribution of low-lying collective or single-particle states $\varepsilon_{fi}^{JK\pi}$ and the second term that from the continuum levels at the saddle deformations, ϵ is the intrinsic excitation energy of fissioning nucleus. The first term contribution due to discrete transition states as well as the total level density $\rho_{fi}(\epsilon, J, \pi)$ of the fissioning nucleus are determined by the order of symmetry of nuclear saddle deformation at inner and outer saddles [24].

In case of axial symmetry at the inner saddle the band-heads spectra are similar to those at equilibrium deformation. For even-even nuclei, in case of axial asymmetry at the inner saddle the $\gamma-$vibration $K^\pi = 2^+$ band-head is sufficiently lowered. The position of negative parity band $K^\pi = 0^-$ at outer saddle is lowered due to mass asymmetry and is almost degenerate with lowest state $K^\pi = 0^+$. Each one-quasiparticle state in odd fissioning nucleus is assumed to have a rotational band built on it with a rotational constant, dependent upon the respective saddle deformation. We construct the discrete transition spectra up to $\sim$100 keV, using one-quasiparticle states by Bolsterli et al. [25] (see [11]). Due to the axial asymmetry at the inner saddle the number of rotational states increases and we additionally assume $(2J + 1)$ rotational levels for each J value. The negative parity bands K^π

$= 1/2^-, 3/2^-, 5/2^-$ ... at outer saddle are assumed to be doubly degenerate due to mass asymmetry.

Theoretical fission barrier height values and saddle order of symmetry are interdependent, the same is the case with our model parameters, i.e. inner and outer fission barrier heights and curvatures E_{fA}, $\hbar\omega_A$, E_{fB}, $\hbar\omega_B$ as well as level densities at both saddles. According to shell correction method calculations for actinides by Howard and Möller [9] the following tendencies regarding E_{fA} and E_{fB} values were anticipated. In case of the actinide nuclei of interest outer fission barrier retains axial symmetry while being mass asymmetric. Inner barrier of higher mass nuclides ($A > A_{tr}$) is triaxially asymmetric during fission process, as has first been noted by Pashkevich [26], while that of lower mass fissioning nuclides ($A \leq A_{tr}$) retains axial symmetry. The transition $A-$value A_{tr} depends on Z and N of fissioning nucleus. It was calculated by Howard and Möller [9] that axially symmetric inner saddle becomes lower than the triaxially asymmetric one by $\sim$1 MeV. This peculiarity would be probed for U, Np and Pu neutron-induced fission cross section data. The most explicit evidence of this peculiarity was encountered in case of ^{232}U(n,f) data analysis. This can explain the non-threshold behavior of measured data at low incident neutron energies [27].

2.3 Level Density

Level density $\rho(U, J, \pi)$ at saddle and equilibrium deformations in adiabatic approximation could be represented as the factorized contribution of quasiparticle and collective states:

$$\rho(U, J, \pi) = K_{rot}(U, J) K_{vib}(U) \rho_{qp}(U, J, \pi), \tag{17}$$

where $\rho_{qp}(U, J, \pi)$ is the quasiparticle level density at excitation energy U, spin J and parity π, $K_{rot}(U, J)$ and $K_{vib}(U)$ are factors of rotational and vibrational enhancement of the level density [13]. Shell and pairing effects influence mainly quasiparticle level density. The collective contribution to the level density of deformed nucleus is defined by the nuclear deformation order of symmetry [24]. The actinide nuclei equilibrium deformation is axially symmetric. The order of symmetry of nuclear shape at inner and outer saddles we adopted from SCM calculations by Howard & Möller [9]. For axially symmetric and axially asymmetric deformations, which are characteristic for equilibrium (outer saddle) and inner saddle deformations of actinide nuclei factors of rotational enhancement could be represented as [24] :

$$K_{rot}^{sym}(U) = \sum_{K=-J}^{K=J} exp(-K^2/K_o^2) \approx \sigma_\perp^2 = F_\perp t, \tag{18}$$

$$K_{rot}^{asym}(U) \simeq 2\sqrt{2\pi}\sigma_\perp^2 \sigma_\parallel, \tag{19}$$

where $\sigma_\perp$ and $\sigma_\parallel$ are the angular momentum distribution parameters, t is the thermodynamic temperature. The mass asymmetry at outer saddle doubles the $K_{rot}^{sym}(U)$ factor as defined above.

Few-quasiparticle effects are essential for state density calculation at low intrinsic excitation energies. An evidence of few-quasiparticle effects at stable deformations in neutron-induced reactions was revealed recently. The step-like structure in ^{239}Pu(n,2n) reaction cross section was shown to be a consequence of threshold excitation of two-quasiparticle configurations in residual even-even nuclide ^{238}Pu [28] above a pairing gap. The same effect is pronounced in ^{238}U(n,γ) data description through (n,γn$'$) reaction competition [29]. The perturbations of the level density by pair correlations was directly evidenced in statistical $\gamma-$decay spectra of even rare-earth nuclei [30, 31].

The estimate of quasiparticle level density $\rho_{qp}(U, J, \pi)$ or intrinsic quasiparticle state density $\omega_{qp}(U)$, could be obtained using Boltzman-gas model prescriptions [28, 32, 33]. The intrinsic state density of quasiparticle excitations $\omega_{qp}(U)$ could be represented as a sum of $n-$quasiparticle state densities $\omega_{nqp}(U)$:

$$\omega_{qp}(U) = \sum_n \omega_{nqp}(U) = \sum_n \frac{g^n (U - U_n)^{n-1}}{((n/2)!)^2 (n-1)!}, \tag{20}$$

where $g = 6a_{cr}/\pi^2$ is a single-particle state density at the Fermi surface, n is the number of quasiparticles. This equation would produce a step-like structure of state density at low excitation energies either for even and odd nuclei. Partial $n-$quasiparticle state densities $\omega_{nqp}(U)$ depend critically on the threshold values U_n for excitation of the n-quasiparticle configurations, $n = 1, 3...$ for odd-A nuclei and $n = 2, 4...$ for even-even or odd-odd nuclei. The discrete character of few-quasiparticle excitations is virtually unimportant only in case of odd-odd nuclei. The values of U_n are defined as proposed by Fu [33]. They depend on shell correction values for saddle and stable deformations and correlation function Δ [17].

Flexible semi-empirical estimate of intrinsic state density $\omega_{qp}(U)$ could be obtained with what we would call "modified Constant Temperature Model (CTM) approach". In this approach the modelling of total level density

$$\rho(U) = K_{rot}^{sym}(U) K_{vib}(U) \frac{\omega_{qp}(U)}{\sqrt{2\pi}\sigma_\parallel} = T^{-1} \exp((U - U_o)/T) \tag{21}$$

where $U_o \simeq -m\Delta$, $m = 0$, 1, 2 for even, odd and odd-odd nuclei, respectively, looks like a simple renormalization of quasiparticle state density $\omega_{qp}(U)$ at excitation energies $U < U_c$. Spin distribution parameter $\sigma_\parallel^2 = F_\parallel t = 6/\pi^2 \langle m^2 \rangle (1 - 2/3\varepsilon) t$, where $\langle m^2 \rangle = 0.24 A^{2/3}$ is the average value of the squared projection of the angular momentum of the single-particle states, and ε is quadrupole deformation parameter. Constant temperature model parameters T, U_c and U_o were obtained for equilibrium deformations by fitting cumulative number of low-lying levels [34]. Constant

temperature model parameters for fission level density might be adopted after following assumptions. The respective constant temperature parameters for fissioning nucleus, namely, nuclear temperature T_f and excitation energy shift U_{of}, are defined at the matching energy $U_{cf} = U_c$, which is adopted to be the same as for equilibrium deformation. That is a fair approximation because for ground state deformations the U_c value is not very much sensitive to the $a-$parameter values. After that the effects of non-axiality and mass asymmetry could be included. At excitation energies above U_{cf} the continuum part of the transition state spectrum is represented with the GSM model [13].

The respective level density parameters for inner(outer) saddle and equilibrium deformations: shell correction δW, pairing correlation function Δ, quadrupole deformation ε, and momentum of inertia at zero temperature $F_o/\hbar^2$. Shell correction values at inner and outer saddle deformations $\delta W_f^{A(B)}$ are adopted following the comprehensive review by Bjornholm and Lynn [7]. For ground state deformations the shell corrections were calculated as $\delta W = M^{exp} - M^{MS}$, where M^{MS} denotes liquid drop mass (LDM), calculated with Myers-Swiatecki parameters [35], and M^{exp} is the experimental nuclear mass. We assume that asymptotic value of main level density parameter $\tilde{a}$ is independent on the deformation of the nucleus, i.e. we use the same values for nuclei at saddle and equilibrium deformations. Note that shell correction is negative at ground state and positive at saddles, consequently a-parameter values at low excitation energies would be rather different. The values of the main $a-$parameter of the model, $\tilde{a}$ and a_{cr}, at high excitations and at excitation energy $U = U_{cr}$, respectively, are defined by fitting neutron resonance spacing [34].

2.4 Fission Cross Section Calculation

Approach adopted here to model level density at equilibrium and saddle deformations was used to describe available neutron-induced fission cross section data for actinide nuclei up to emissive fission threshold. Above ~2.5 MeV incident neutron energy fission cross section data were fitted by slight increase of pairing correlation function value Δ_f. Actually the amount of this increase depends on the ratio of $a-$parameters at saddle and equilibrium deformations, which, in turn, is a function of $(\delta W_f^{A(B)} - \delta W)$. It might be anticipated that value of the parameter $\delta = (\Delta_f - \Delta)$ contains lumped effect of pairing and shell effects differences at saddle and equilibrium deformations. At lower energies few-quasiparticle effects in level density seem to be important.

2.4.1 Z-even, N-odd fissioning nuclei

In case of Z-even, N-even targets fission cross section data for U ($A \geq 234$), Pu ($A \geq 238$) and Cm target nuclei exhibit almost classic threshold shape. In case of ^{232}U and ^{236}Pu target nuclides there is a non-threshold behavior in contrast with other N-

even isotopes. SCM calculations by Howard & Möller [9] predicted axial symmetry of inner fission barrier, while $E_{fA} < E_{fB}$, for neutron-deficient odd uranium and plutonium nuclei with $A \leq 235$ and $A \leq 237$, respectively. This helps to correlate this non-threshold behavior with theoretical fission barrier parameter trends [27]. In case of other plutonium and curium targets neutron-induced fission cross sections the step-like and resonance-like structures, respectively, are observed above fission threshold, so that a region traditionally called 'first plateau' starts at ~2.5-3 MeV. They are supposed to be due to interplay of one-quasiparticle excitations in the level density of odd fissioning nucleus and two-quasiparticle excitation in even-even residual nucleus [17]. Step, evident in ^{238}Pu(n,f) measured data (see Fig. 1) could be interpreted by modelling fission level density for ^{239}Pu.

In odd nuclei "blocking" of pairing by unpaired particle is roughly taken into account by excitation energy shift. The level density of the fissioning nuclide ^{239}Pu could be calculated with Eqs. (17-20), introducing odd-even excitation energy shift: $\widetilde{U} = U + \Delta$, where Δ is the correlation function for the saddle point deformations. At lower energies the energy behavior of level density is strongly dependent on the number of excited quasiparticles. Pairing is weakened by excitation of few-quasiparticle states, so virtually only lowest quasiparticle number states lead to pronounced structure in level density of actinide nuclei. In case of even-odd fissioning nuclide ^{239}Pu the partial contributions $\omega_{nqp}(U)$ of $n-$quasiparticle states to the total intrinsic state density $\omega_{qp}(U)$ produce "shoulder" below three-quasiparticle state excitation threshold. For the lowest number of quasiparticles n =1 intrinsic state density $\omega_1 \sim g$ and there is no explicit excitation energy dependence within Boltzman-gas model approximation. One-quasiparticle state density defines the step-like trend of fission cross section up to the incident neutron energy of $E_3 = U_3 + E_{fA} - B \simeq 1.25$ MeV, where B is the neutron binding energy, E_{fA} is the inner saddle height, which corresponds to three-quasiparticle state excitation threshold U_3 at the inner saddle deformation. At higher incident neutron energies the three-quasiparticle state excitations with intrinsic excitation state density $\omega_3 \sim g^3U^2$ came into play. Hence, the fission cross section starts to increase once again above three-quasiparticle state excitation threshold (see Fig. 1).

In this excitation energy region we will model the level density as

$$\begin{aligned} \rho(U) &= T_f^{-1}(1 + \delta_{10}(U - 0.5U_3)) \exp((U_3 + \Delta_f - U_o - \delta_1)/T_f) \\ &\simeq T_f^{-1} \exp((\Delta_f - U_o)/T_f). \end{aligned} \qquad (22)$$

Using this equation we could fit measured fission cross section data trend using parameters $\delta_1 = 1.25$ MeV and $\delta_{10} = 2$ MeV, which model one-quasiparticle state density. One- and three-quasiparticle states level density of even-odd fissioning nucleus ^{239}Pu defines the fission cross section shape at incident neutron energies below ~2.5 MeV. For excitation energies below five-quasiparticle and above three-quasiparticle states excitation threshold the level density could be slightly increased

as compared with constant temperature model approximation, to produce a better data fit:

$$\rho(U) = T_f^{-1} \exp((U - U_o + \delta_3)/T_f), \tag{23}$$

where value of the parameter $\delta_3 = 0.145$ MeV was defined by fitting fission cross section data. Level density of fissioning nuclide ^{239}Pu at inner saddle, triaxiality effects being included, is shown on Fig. 2. Calculated level density is compared with constant temperature approximation and "scaled" Boltzman-gas model, which also fits fission data. The arrows on the horizontal axis of Fig. 2 indicate the excitation thresholds of odd $n-$quasiparticle configurations.

Fission cross section data of ^{238}U (Fig. 3) exhibit almost classic threshold shape, since vibrational resonance at ~1.15 MeV is rather weak, while "cusp" in fission cross section around 3.3 MeV incident neutron energy [20] might be correlated with excitation of three-quasiparticle states in fissioning nuclide ^{239}U above 2.4 MeV. At this high excitation energy influence of one-quasiparticle states on calculated fission cross section starts to diminish. There are also some peculiarities in fission cross section data of ^{236}U and ^{234}U below ~2 MeV incident neutron energies, besides strong vibrational resonances at ~0.93 MeV in ^{236}U(n,f) and 0.78 MeV in ^{234}U(n,f). Adopted level density description allows to fit subthreshold cross section shape of ^{236}U(n,f) and ^{234}U(n,f). Note that for ^{237}U and ^{239}U fissioning nuclides $E_{fA} > E_{fB}$, while for ^{235}U and ^{233}U $E_{fA} < E_{fB}$. Incident neutron energies $E_3 = U_3 + E_{fA(B)} - B$ correspondent to excitation of three-quasiparticle states are: ~ 2.3 MeV for ^{238}U(n,f), ~1.8 MeV for ^{236}U(n,f), ~1.2 MeV for ^{234}U(n,f) and ~0.7 MeV for ^{232}U(n,f). Approximately at these energies, which are above fission threshold, abrupt changes in cross section shapes are observed.

In this section sensitivity of calculated fission cross section to one- and three-quasiparticle state density of fissioning nucleus was estimated by changing values of $|\delta_1|$ and $|\delta_3|$ by 0.1 MeV. Dashed and short-dashed curves on Figs. 1, 3 and 4 show the sensitivity of calculated fission cross section to one– and three-quasiparticle excitations in fissioning nuclide. In case of ^{238}U(n,f) reaction above ~2.3 MeV incident neutron energy three-quasiparticle excitations occur (see Fig. 3), but calculated fission cross section is much more sensitive to one–quasiparticle state density variation in fissioning nuclide ^{239}U.

Excitation of three-quasiparticle states in fissioning nucleus is more pronounced for neutron-induced reactions on Pu target nuclei. Dashed and dot-dashed curves of Fig. 1 show the sensitivity of calculated fission cross section to the level density of ^{239}Pu fissioning nuclide at excitation energies lower than three-quasiparticle excitation threshold. For dashed curve, in fact, one-quasiparticle state density is varied, i.e. level density $\rho(U)$ is calculated with $\delta_1 = 1.35$ MeV (see Eq.(22)), while for solid curve $\delta_1 = 1.25$ MeV. Calculated fission cross section appears to be slightly sensitive to one-quasiparticle state density below 1 MeV incident neutron energy, while it is very sensitive above 1 MeV up to 3 MeV.

Fission cross section of ^{240}Pu also exhibits step-like irregularity above ~1 MeV incident neutron energy. Incident neutron energies E_3 ~1.5 MeV for ^{240}Pu(n,f), for other plutonium targets they are: ~ 1.25 MeV for ^{238}Pu(n,f), ~1.6 MeV for ^{242}Pu(n,f) and ~1.7 MeV for ^{244}Pu(n,f).

The most striking peculiarity in fission cross section data above fission threshold are quasi-resonance structures, evident in fission cross section data by Fursov et al. [36], Moore et al. [37] and Fomushkin et al. [38, 39] for ^{244}Cm(n,f), ^{246}Cm(n,f), ^{248}Cm(n,f) reaction cross sections, although there are a systematic discrepancies evident in data sets as regards either data shapes and absolute values [11]. Broad quasi-resonance structure around 1.4 MeV neutron energy, evident in measured data by Fomushkin et al.[38] and by Fursov et al. [36] (see Fig. 4). These data could be described in the same manner as those for Pu even-even target nuclei. Here, in case of even-odd fissioning nuclide ^{247}Cm partial contributions $\omega_{nqp}(U)$ of $n-$quasi-particle states to the total intrinsic state density $\omega_{qp}(U)$ produce "jumps" again only for n =1 and n =3. We suppose that ^{242,244,246,248}Cm target cross sections magnitudes are governed by the inner fission barrier, parameters of which are fixed by fission data fit for incident neutron energy above ~10 keV. One-quasiparticle state excitation define the decreasing trend of fission cross section above fission barrier up to the incident neutron energy of $E_3 = U_3 + E_{fA} - B$. Figure 4 shows the sensitivity of calculated fission cross section to one- and three-quasiparticle state density. Fission cross section shape up to 2.5 MeV neutron energy is controlled mainly by one-quasiparticle state density, while three-quasiparticle state density is important in the energy range of 2-3.5 MeV.

The modelling of the intrinsic state density structure of fissioning and residual nuclei has enabled the qualitative analysis of the quasi-resonance structure in ^{244}Cm(n,f), ^{246}Cm(n,f), ^{248}Cm(n,f) measured data well-above fission threshold. This irregularity is the consequence of threshold excitation of three-quasiparticle configurations. The excitation threshold is consistent with measured data below fission threshold [40].

Plotting values of $E_{fA(B)} + U_3 - B_n$, three-quasiparticle excitation threshold in neutron energy scale as a function fissioning nucleus mass A, one may notice that they are correlated with evidence of two-quasiparticle effects in U, Pu and Cm neutron-induced fission cross sections. The one-quasiparticle neutron states of even-odd fissioning nuclide, lying below the three-quasiparticle states excitation threshold define the shape of fission cross section below incident neutron energy of $E \leq E_{fA(B)} + U_3 - B_n$. At higher excitation energies three-quasiparticle states are excited. Two-quasiparticle states in even residual nucleus could be excited at incident neutron energies $E > U_2$. Relative position of U_3 and U_2 excitation thresholds in fissioning and residual nuclei, respectively, might influence fission cross section shape below ~3 MeV incident neutron energy.

Adopting structureless constant temperature approximation of level density one could describe the fission cross section data only above 3-4 MeV incident neutron

energy and deep below fission threshold, when fission transmission coefficient is defined mainly by discrete fission transition states. At intermediate incident neutron energy, that is the energy range where excitation of few-quasiparticle states at the inner saddle is of primary importance, structureless constant temperature approximation fails.

2.4.2 Z-even, N-even fissioning nuclei

In case of Z-even, N-odd fissile targets the step-like irregularities in fission cross section data shapes below ~2 MeV are supposed to be due to interplay of two-quasiparticle excitations in the level density of even-even fissioning nucleus and one-quasiparticle excitation in odd$-A$ residual nucleus. The collective levels of even fissioning nuclei, lying within pairing gap, define the fission cross section below incident neutron energy of $E \leq E_{fA(B)} + U_2 - B_n$, where $E_{fA(B)}$ is the higher of the barrier humps. At excitation energies $U > U_2$, i.e. above the pairing gap, level density of axially symmetric fissioning nucleus is calculated as described below. After that the effects of mass asymmetry at the outer saddle are included.

The most distinct evidence of pair correlation effects is observed in case of ^{233}U(n,f) (see Fig. 5) and ^{235}U(n,f) reactions. SCM calculations by Howard & Möller [9] predicted that inner fission barrier for uranium nuclei with $A \leq 236$ is axially symmetric while $E_{fA} < E_{fB}$. In case of Pu and Cm nuclei addressed here the higher barrier is the inner one. The two-quasiparticle excitations in ^{234}U at the outer saddle deformations occur at intrinsic excitation energy, correspondent to $E \geq 0.1$ MeV, they explain the step-like behavior of ^{233}U(n,f) data shape above 0.1 MeV up to 2 MeV.

In case of even-even nuclides the partial contributions of $\omega_{nqp}(U)$ of $n-$quasiparticle states to the total intrinsic state density $\omega_{qp}(U)$ produce "jumps" only for $n = 2$ and $n = 4$ configurations (see Fig. 6). The arrows on the horizontal axis of Fig. 6 indicate the excitation thresholds of even $n-$quasiparticle configurations. The intrinsic state density $\omega_2(U)$ for the residual nuclide ^{234}U could be represented by equation, modifying Boltzman-gas approximation of $\omega_2(U) = g^2(U - U_2)$ with a Woods-Saxon expression at excitations below four-quasiparticle excitation threshold:

$$\omega_2(U) = g^2(U_4 - U_2 - 0.35)(1 + \exp((U_2 - U + 0.1)/0.1))^{-1}. \quad (24)$$

Almost the same estimate of two-quasiparticle states $\omega_2(U)$ was obtained by modelling the structure of ^{238}Pu intrinsic state density to interpret the step-like structure in ^{239}Pu(n,2n) reaction data near threshold [28]. We model here the nuclear level density $\rho(U)$ in the same manner as for ^{239}Pu nuclide. Above the pairing gap U_2 up to the four-quasiparticle excitation threshold U_4 level density is approximated as

$$\rho(U) = \rho(U_4 - \delta_2)/(1 + \exp(U_2 - U + \delta_a)/\delta_s), \quad (25)$$

here $\delta_2 \sim 0.5(U_4 - U_2)$. Two-quasiparticle states level density of even-even fissioning nuclide ^{234}U influences the fission cross section shape at incident neutron energies above ~0.1 MeV. Parameters $\delta_2 = 0.55$ MeV, $\delta_a = \delta_s = 0.1$ MeV, which define two-quasiparticle states level density values were extracted by fitting measured fission data. Calculated level density is compared with constant temperature approximation and "scaled" Bose-gas model (see Fig. 6). Present and Boltzman-gas approximation are consistent at low excitation energies, while they start to be discrepant around 5 MeV excitation energy.

In this section sensitivity of calculated fission cross section to two- and four-quasiparticle state density of fissioning nucleus was estimated by changing $|\delta_2|$ and $|\delta_4|$ by 0.2 MeV. Dashed and short-dashed curves on Fig. 5 show the sensitivity of calculated fission cross section to two-and four-quasiparticle excitations in fissioning nuclide ^{234}U. Above ~0.9 MeV incident neutron energy four-quasiparticle excitations occur (see Fig. 5), but calculated fission cross section is much less sensitive to relevant state density variation. At intrinsic excitation energies higher than four-quasiparticle excitation threshold U_4 level density $\rho(U)$ was estimated as

$$\rho(U) = T_f^{-1} \exp((U_6 - U_o - \delta_4)/T_f), \tag{26}$$

where U_6 is six-quasiparticle excitation threshold, $\delta_4 = 0.2$ MeV. Fission level density of ^{234}U is shown on Fig. 6. The arrows on the horizontal axis of Fig. 6 indicate the excitation thresholds of even $n-$quasiparticle configurations.

In case of ^{235}U(n,f) cross section two-quasiparticle states at outer saddle of ^{236}U fissioning nuclide are excited at higher incident neutron energies, as compared with respective excitation threshold in ^{233}U(n,f) reaction. It corresponds to $E \geq 0.6$ MeV, here also a step-like behavior of data shape is observed [16]. Above ~1.4 MeV incident neutron energy four-quasiparticle excitations occur, calculated fission cross section here is more sensitive to relevant four-quasiparticle state density variation. That is due to higher fission threshold of ^{236}U as compared with fission threshold of ^{234}U.

In case of ^{234}U and ^{236}U fissioning nuclides the inner barrier of fissioning nuclides is lower than outer one, in case of Pu, Cm and Cf nuclei addressed here the higher barrier is the inner one. That means that we can fix basically the discrete transition spectra at outer saddle fitting ^{233}U(n,f) and ^{235}U(n,f) data. The discrete transition spectra at inner saddle could be fixed fitting ^{239,241}Pu(n,f), ^{243,245,247}Cm(n,f) and ^{249}Cf(n,f) measured data.

Values of δ_2 and δ_4 parameter values fluctuate only slightly for various U, Pu and Cm nuclei. Adopting structureless constant temperature approximation of fission level density one fails to describe fission cross section of Z-even, N-odd fissile targets exactly in the neutron energy range up to ~2-3 MeV incident neutron energy. Evidence of few-quasiparticle excitation depends on the fission barrier value in the neutron energy scale. At intrinsic excitation energies $U \geq U_6$ fission level density is almost perfectly smooth.

2.4.3 Z-odd, N-even fissioning nuclei

In case of the only available data for Z-odd, N-odd target ^{242m}Am the effect of Z-odd, N-even fissioning nucleus level density is evidenced as a step-like shape of fission cross section data. The one-quasiparticle neutron states of odd-even ^{243}Am fissioning nuclide define the shape of ^{242m}Am(n,f) fission cross section below incident neutron energy of ~1 MeV. Specifically, the step-like shape of fission cross section around 0.1 - 0.4 MeV [32]. At higher incident neutron energies three-quasiparticle states could be excited in fissioning nucleus ^{243}Am at deformations of inner fission barrier hump. They define the fission cross section shape around 1 - 2.5 MeV incident neutron energy. There is virtually no step-wise structure in level density of odd-odd residual nuclide ^{242}Am. Calculated fission cross section appears to be less sensitive to one-quasiparticle state density, than fission cross section of Z-even, N-even targets, because of high fissility of ^{243}Am nuclide.

3 Cross section above emissive fission threshold

3.1 Fission cross section

At incident neutron energies higher than ~5-6 MeV, when fission reaction of A, $A-1$ and $A-2$ compound nuclides is possible after emission of 1, 2 or 3 neutrons, the observed fission cross section is a superposition of non-emissive or first chance fission of nucleus A and xth-chance fission contributions. These contributions are weighted with a probability of x neutrons emission before fission. In case of neutron-induced fission of ^{238}U target nuclide, for fixed statistical model parameters (i.e. level density and fission barrier parameters) of residual nuclei ^{238}U, ^{237}U or ^{236}U, fissioning in (n,nf), $(n,2nf)$ or $(n,3nf)$ reactions, respectively, the behavior of the first-chance fission cross section σ_{f1} should make it possible to reproduce the measured fission cross section σ_f of ^{238}U up to 20 MeV incident neutron energies. This approach is realized in a STAPRE [41] code, which was used for present calculations. Fission at this excitation energies is an equilibrium process, so it is assumed that it does not compete with pre-equilibrium particle emission. First chance fission cross section is defined as

$$\sigma_{nf}(E) = q(E)\frac{\pi\,\lambda\!\!\!^{-2}}{2(2I+1)}\sum_{lJ}(2l+1)T_l(E)P_f^{J\pi}(E)S_{nf}^{J\pi}, \qquad (27)$$

where $q(E)$ is the fraction of first composite nuclide, which survives the pre-equilibrium emission of first neutron, l is the orbital momentum of incident neutron, $T_l(E)$ is the transmission coefficient. Contributions of (n,nf), (n,2nf) and (n,3nf) reactions of equilibrated nuclei to the observed fission cross section are calculated using fission probability estimates $P_{fi}^{J\pi}(U)$ for ith compound nuclides ^{238}U ^{236}U and ^{235}U as

$$\sigma_{ninf}(E) = \sum_{J\pi} \int_0^{U_{max}} W_i^{J\pi}(U) P_{fi}^{J\pi}(U) dU \tag{28}$$

where $W_i^{J\pi}(U)$ is the cumulative population of ith compound nucleus. Contributions of (n,nf), (n,2nf) and (n,3nf) reactions correspond to neutron-induced fission cross sections of ^{237}U(n,f), ^{236}U and ^{235}U.

A consistent description of the most complete set of measured data on the (n, f), $(n, 2n)$, $(n, 3n)$ and $(n, 4n)$ reaction cross sections for the ^{238}U target nuclide up to 20 MeV enables one to consider the estimates of σ_{f1} and fission probability $P_{f1}$of the initial compound nuclei ^{239}U as fairly realistic. Fission cross section of ^{238}U, shown on the Fig. 7, demonstrates a step-like structure, relevant to contribution of (n,$i$nf) reactions to total fission cross sections for i = 1, 2, 3. Contribution of first-chance fission appears to be sensitive to level density of residual nuclide ^{238}U. Contribution of second- chance fission of ^{238}U compound nuclide is sensitive to level density of fissioning nuclide ^{238}U. Estimate of ^{237}U $\langle D_{obs} \rangle$ = 2.973±0.416 eV, obtained by analysis of resolved resonance parameters [34] is consistent with preequilibrium contribution into first neutron spectrum [42] and subsequent sharing of $\sigma_r = \sigma_{n,f1} + \sigma_{n,nx}$ reaction cross section into first-chance fission and neutron emission cross sections. To get a consistent fit of measured cross sections up to 20 MeV we decreased $\tilde{a}_f$ of fissioning nuclide ^{238}U by ~10%.

3.2 Secondary neutron spectra

Shape of calculated (n,2n) reaction cross section, especially it's high-energy tail, is strongly correlated with secondary neutron spectrum shape. Cross section of (n,3n) reaction is less sensitive to pre-equilibrium neutron emission contribution. The hard component of neutron scattering spectra and high energy tail of ^{238}U$(n, 2n)$ reaction cross section are interpreted as being due to the pre-equilibrium evaporation of neutrons [43, 12, 42]. This feature is parameterized within a conventional exciton model, used in STAPRE [41] code. By fitting the measured spectra [44] for $E_n = 6 - 14.7\ MeV$ we get the main parameter of the exciton model, that is the matrix element $M^2 = 10/A^3$. Note that, when calculating the exciton state density, the odd-even back-shift is introduced: $\hat{U} = U - \Delta(2 - n)$. The charge conservation and transition rates renormalization were also employed. With all that in mind and in the STAPRE code [41] a pre-equilibrium emission fraction $q(E)$ leading to depletion of compound nucleus states population is obtained, which approaches ~0.45 at E_n = 20 MeV. Largely by diminishing the odd-even dependence of $q(E)$ we can fit the ^{235}U fission data with the same M^2 value. These reasonable model fits give rather strong grounds to consider the estimate of contribution of first neutron pre-equilibrium emission $q(E)$ as fairly realistic. They were used also for interpreting the experimental evidence of preequilibrium neutron emission prior to neutron-induced fission of ^{238}U, induced by 14.7 MeV neutrons [42].

Figures 7 and 8 show what happens when one ignores pre-equilibrium emission of first neutron completely in case of ^{238}U(n,f) and ^{235}U(n,f) reactions. The main effect is in first-chance fission cross section, which starts increasing wildly, as well as total fission cross section, above (n,nf) reaction threshold. Contributions of (n,nf) and (n,2nf) reactions to the total fission cross sections are not affected that much. Consequently, inelastic scattering cross section would go to zero abruptly, as well as $^{238}\mathrm{U}(n,2n)$ reaction cross section, which starts decreasing steeper, than measured data predict, above 13 MeV incident neutron energy. Shape of $^{238}\mathrm{U}(n,3n)$ reaction cross section also becomes deteriorated.

3.3 Shell effects in first chance fission cross section

The behavior of the first-chance fission cross section σ_{nf} is obviously related with the energy dependence of the first-chance fission probability of the $A+1$ nucleus P_{f1}:

$$\sigma_{nf} = \sigma_r(1-q(E))P_{f1}. \tag{29}$$

Once the contribution of first neutron pre-equilibrium emission $q(E)$ is fixed, the first-chance fission probability P_{f1} depends only on the level density parameters of fissioning a_f and residual a_n nuclei. That is, actually it depends on the shell correction values $\delta W_{fA(B)}$ and δW_n. The values of the shell corrections as well as of the fission barriers, obtained with different theoretical calculations, vary by $1 \sim 2$ MeV. The same is true for the experimental shell corrections, which are obtained with a smooth component of potential energy calculated according to the liquid-drop or droplet model. However the isotopic changes of $\delta W_{fA(B)}$ and δW_n [7] are such that first-chance fission probability P_{f1} viewed as a function of the difference $(\delta W_{fA(B)} - \delta W_n)$ is virtually independent on the choice of smooth component of potential energy. In addition, existing calculations of the shell corrections do not allow for the influence of the asymmetric deformations on the smooth component of potential energy. Therefore, we shall consider the adopted $\delta W_{fA(B)}$ estimates to be effective, provided that δW_n are obtained with the liquid drop model. The trend of the first-chance fission cross section σ_{nf} shown in Figs. 9, 10 for ^{238}U(n,f) and ^{235}U(n,f) reactions could be treated as a manifestation of the shell effects in first chance fission probability. So it can be stated that we have got effective estimate of σ_{f1} which corresponds to consistent fit of $(n,2n)$, $(n,3n)$ and $(n,4n)$ reaction cross section data. Figures 9 and10 shows also the damping of shell effects in fissioning nuclei ^{239}U and ^{236}U with excitation energy. Decreasing shell correction value for the outer saddle deformations by 2 MeV, we get rather steeply decreasing first-chance fission cross section and deteriorated shapes of total fission and (n,2n) and (n,3n) reaction cross sections. Contributions of (n,nf) and (n,2nf) reactions remain almost unchanged. In case of ^{238}U(n,f) reaction slight discrepancy of calculated and measured data below emissive fission threshold could be easily removed by

small variation of E_{fA} or E_{fB} fission barrier parameters, which would not affect first-chance and total fission cross sections above ~10 MeV. This marked change of outer saddle shell correction δW_B produces almost linear decrease of first-chance fission cross section of ^{235}U(n,f) reaction (see Fig. 9), total fission cross section being almost unchanged.

Summarizing, we argue that we have got effective estimates of first-chance fission probabilities $P_{f1}$and pre-equilibrium emission fraction $(1 - q(E))$ for the first neutron spectrum. Consequently, we could describe measured neutron-induced fission data up to 20 MeV incident neutron energies for target nuclei with various fissilities and parities of protons Z and neutrons N. It seems that present estimates of fission barrier parameters and fission level density modelling provide a consistent description of available data up to 20 MeV.

4 Fission barriers

The collective contribution to the level density of deformed nucleus is determined by the order of symmetry of nuclear shape deformation at saddles [13]. The collective effects are manifested as drastic sensitivity to the inclusion of inner saddle point triaxiality of both experimental and theoretical fission barrier parameters. The theoretical SCM fission barriers depend on elongation as well as axially symmetric and asymmetric coordinates. Introducing or abandoning saddle asymmetries relevant to SCM calculations we observe that fission barriers, extracted by cross section data analysis also exhibit strong (Z, N)-dependence [14, 15]. Once again, the non-threshold energy dependence of the ^{232}U(n,f) cross section is interpreted in a double-humped fission barrier model [27], the inner barrier of fissioning nucleus ^{233}U being ~ 1 MeV lower than the outer one, as anticipated with the SCM calculation [9]. The inner barrier was assumed axially symmetric in case of U compound systems with $A \leq 236$ and asymmetric for $A > 236$.

Fission barrier parameters: inner(A) and outer(B) barrier heights $E_{fA(B)}$ and curvatures $\hbar\omega_{A(B)}$ are given in Table 8 of [11]. Provided values of correlation function $\Delta_f = \Delta_o + \delta$ at saddles depends, actually, on a_f/a_n ratio, which is a function of $(\delta W_f - \delta W_n)$. The comparison of obtained U, Np, Pu, Am, Cm fission barriers with SCM fission barriers and fission barriers provided by Smirenkin [45] shows that for uranium the agreement is rather good for outer fission barrier. As regards the inner barrier the isotopic dependences of present barriers and those predicted by Smirenkin [45] are similar. For plutonium and americium nuclei the agreement would be also good, if not the americium outer barrier for neutron-deficient nuclei. However, we extracted these barrier values by analysis of emissive fission contribution for the reaction ^{241}Am(n,f), which seems to be less reliable than analysis of relevant fission cross section below emissive fission threshold. Most disturbing might be the discrepancy in case of curium outer barrier values, measured data base have changed extensively during recent years and this is reflected in

present fission barrier parameters.

4.1 Do we really need non-axiality and mass asymmetry at saddles

Calculated fission cross section appear rather sensitive to the fission barrier parameter values and we could estimate their uncertainties at rather low level: $\delta E_{fA} \sim 0.05$ MeV, $\delta E_{fB} \sim 0.10$ MeV, $\delta\hbar\omega_A \sim 0.03$ MeV, except curvature of outer fission barrier hump, where $\delta\hbar\omega_B \sim 0.4$ MeV. These uncertainties were defined as uncorrelated sensitivity of calculated fission cross section to the respective parameter variation, as compared with measured data base. Introducing or abandoning non-axiality or mass asymmetry at inner and outer saddles, respectively, influences on calculated fission cross section greatly. Figure 11 shows what happens when axial asymmetry is assumed at the inner saddle of ^{239}Pu fissioning nucleus. Calculated fission cross section decreases ~3 times below and ~2 times above fission threshold. It seems to be impossible to compensate this variation of energy dependence by large decrease of inner barrier height δE_{fA} ~1 MeV, since it influences to a larger extent fission cross section below fission threshold. Figure 12 shows what happens when mass asymmetry is assumed at the outer saddle of ^{239}Pu fissioning nucleus. Now calculated fission cross section remains almost unchanged below fission threshold, while it is decreased almost uniformly at higher incident neutron energies. Fortunately, this variation of energy dependence could be easily compensated by $\delta E_{fB} \sim 0.3$ MeV decrease of outer barrier height, since calculated fission cross section is almost insensitive to inner barrier height variation below 1 MeV. For other fissility or parity of number of neutrons N nuclides the sensitivity fashion remains the almost the same. It changes only when outer barrier is higher than the inner one, which is assumed to be axially symmetric and rather low (^{234}U in ^{233}U(n,f) reaction). Axial asymmetry at inner saddle seems to be justified to more extent than mass asymmetry at outer saddle. At excitation energies higher than emissive fission threshold axial asymmetry factors influence first chance fission cross section shape.

Figure 13 shows decreasing ^{239}U inner barrier height E_{fA} by ~1 MeV we could compensate lowering of ^{238}U fission cross section only below emissive fission threshold, at higher excitation energies linear decrease of first chance fission cross section results in drastic lowering of total fission cross section, while (n,nf) and (n,2nf) reaction contributions remain almost the same.

Summarizing, we argue that extracted fission barrier parameters as well as calculated fission cross section shapes up to 20 MeV are consistent with assumption of non-axiality of inner saddle of fission barrier.

5 Conclusions

We investigated the manifestation of a few-quasiparticle effects in fission cross sections. For particular nuclide it depends on the structure of fission barrier of compound nucleus, i.e. on the relative values of inner E_{fA} and outer E_{fB} fission barrier humps and neutron binding energy. The internal excitation energy at the saddle point corresponding to the higher barrier hump $E_{fA(B)}$ is important, basically the value of $(B_n + E - E_{fA(B)})$ matters. We argue that to describe neutron-induced fission cross section data at low energies for even-even and even-odd target nuclei, typically below ~2 MeV incident neutron energy, fission level density at low intrinsic excitation energy is of primary value.

The statistical Hauser-Feshbach model calculations of neutron-induced reaction for ^{238}U and ^{235}U target nuclides show the fair description of available data base on fission and neutron emission cross sections up to 20 MeV incident neutron energy. The rigid rotator coupled channel model gives fair description of available total and differential cross section data. It was observed that contribution of non-emissive fission to the total fission cross section depends on fissility of target nucleus and incident particle. Evaporation/fission mechanism is valid in this excitation energy range. We have shown the importance of inner saddle point non-axiality for obtaining consistent fission barrier and fission cross section estimates.

The sophistication of the level density model, as compared with various options of Fermi-gas closed-form expressions, although it still remains rather crude, seems to be unavoidable, since it is backed by a lot of experimental data. That is the shortest way to consistent modelling of fission cross section data behavior and extracting reasonable level density and fission barrier parameter values.

References

[1] Strutinsky V.M. Nucl. Phys. A95, 420 (1967).

[2] Flerov G.N., Pleve A.A., Polikanov S.M. Nucl. Phys., A97, 444 (1967).

[3] Back B.B., Hansen O., Britt H.C. et al. Phys. Rev., 9, 1924 (1974).

[4] James G.D., Dabbs J.W.T., Harvey J.A. et al., Phys. Rev., C15, 2083 (1977).

[5] Trochon J. et al. Proc. IAEA Conf. on Nuclear Data for Reactors, Helsinki, 1970, v. 1, p.495.

[6] Back B.B., Britt H.C., Hansen O. et al. Phys. Rev., 10, 1948 (1974).

[7] S. Bjornholm and J.E. Lynn, Rev. Mod. Phys. 52 (1980) 725.

[8] Weigmann H.Neutron-Induced Fission Cross Sections, in:The Nuclear Fission Process, ed. C. Wagemans (CRC Press, Boca Raton, 1991) 64.

[9] Howard W.M., Möller P. Atomic Data and Nuclear Data Tables,25, 219 (1980).

[10] Handbook for calculations of nuclear reaction data, IAEA-TECDOC-1034, Vienna, 1998.

[11] Maslov V.M. INDC(BLR)-013, IAEA, Vienna, 1998.

[12] Ignatyuk A.V., Maslov V.M., Pashchenko A.B. Sov. J. Nucl. Phys., 47, 224 (1988).

[13] Ignatjuk A.V., Istekov K.K., Smirenkin G.N. Sov. J. Nucl. Phys. 29, 450 (1979).

[14] Ignatjuk A.V., Maslov V.M., Proc. Int. Symp. Nuclear Data Evaluation Methodology, Brookhaven,USA, October 12-16, 1992, p.440, World Scientific, 1993.

[15] Maslov V.M., Kikuchi Y., JAERI-Research 96-030, 1996.

[16] Ignatyuk A.V., Maslov V.M. Sov. J. Nucl. Phys., 54, 392 (1991).

[17] Maslov V.M. IV International Seminar on Interaction of Neutrons with Nuclei, Dubna, Russia, April 27-30, 1996, p. 65, 1996.

[18] Hauser W. and Feshbach H., Phys. Rev. 87, 366 (1952).

[19] Moldauer P.A., Rev. Mod. Phys. Phys. 36, 1079 (1964).

[20] Maslov V.M., Porodzinskij Yu.V., Hasegawa A. and Shibata K., JAERI-Research, 98-040, 1998.

[21] Shpak D.L., Ostapenko Yu.B., Smirenkin G.N., Sov. J. Nucl. Phys., 13, 547 (1971).

[22] Tepel J.W., Hoffman H.M., Weidenmuller H.A. Phys. Lett. 49, 1 (1974).

[23] Lynn J.E., Back B.B. J. Phys. A: Math., Nucl., Gen., 7, 395 (1974).

[24] Bohr A. and Mottelson B., Nuclear Structure, vol. 2, (Benjamin, New-York, 1975).

[25] Bolsterli M., Fiset E.O., Nix J.R., Norton J.L. Phys.Rev., C 5, 1050 (1972).

[26] Pashkevich V.V., Nucl. Phys. A133, 400 (1969).

[27] Maslov V.M., Kikuchi Y. Nucl. Sci. Eng 124, 492 (1996).

[28] Maslov V.M. Zeit. Phys. A, Hadrons & Nuclei, 347, 211 (1994).

[29] Maslov V.M., Proc. Ninth Int. Symp. Capture Gamma-Ray Spectroscopy and Related Topics, Budapest, Hungary, October 8-12, 1996, p.676.

[30] Dossing T., Khoo T.I., Lauritsen T. et al., Phys. Rev. Lett., 75, 1276 (1995).

[31] Khitrov V.A., Sukhovoj A.M., Voinov A.V., IV International Seminar on Interaction of Neutrons with Nuclei, Dubna, Russia, April 27-30, 1996, p. 45, 1996.

[32] Maslov V.M , Proc. of International Conference on Nuclear Data for Science and Technology, Trieste, Italy, 19-24 May 1997, p.1320.

[33] Fu C. Nucl. Sci. Engng. 86, 344 (1984).

[34] Maslov V.M. and Porodzinskij Yu.V. JAERI-Research, 98-038, 1998.

[35] Myers W.O., Swiatecky W.J., Ark. Fyzik, 36, 243 (1967).

[36] Fursov B.I., Polynov V.N., Samylin B.F., Shorin V.S., Proc. of International Conference on Nuclear Data for Science and Technology, Trieste, Italy, 19-24 May 1997, p.488.

[37] Moore M.S., Keyworth G.A. Phys. Rev. C, 3, 1656 (1971).

[38] Fomushkin E.F., Novoselov G.F., Vinogradov Yu.I., Gavrilov G.F., Zherebtsov Sov. J. Nucl. Phys. 31, 19 (1980).

[39] Fomushkin E.F., Novoselov G.F., Vinogradov Yu.I., Gavrilov G.F., Zherebtsov Sov. J. Nucl. Phys. 36, 338 (1982).

[40] Maguire Jr.H.T.,Stopa C.R.S., Block R.C. et al. Nucl. Sci. Eng. 89, 293 (1985).

[41] Uhl M. and Strohmaier B., IRK-76/01, IRK, Vienna (1976).

[42] Boykov G.S., Dmitriev V.D., Kudyaev G.A., Maslov V.M., et al., Ann. Nucl. Energy, 10, 585 (1994).

[43] Maslov V.M., Porodzinskij Yu.V.,Sukhovitskij E.Sh., Proc. Int. Conf. on Neutron Physics, 14-18 Sept., Kiev, USSR, Vol.1, p.413, 1988.

[44] Kornilov N.V., Yadernie Konstanti, 4, 46 (1985).

[45] Smirenkin G.N., INDC(CCP)-359, Vienna, 1993.

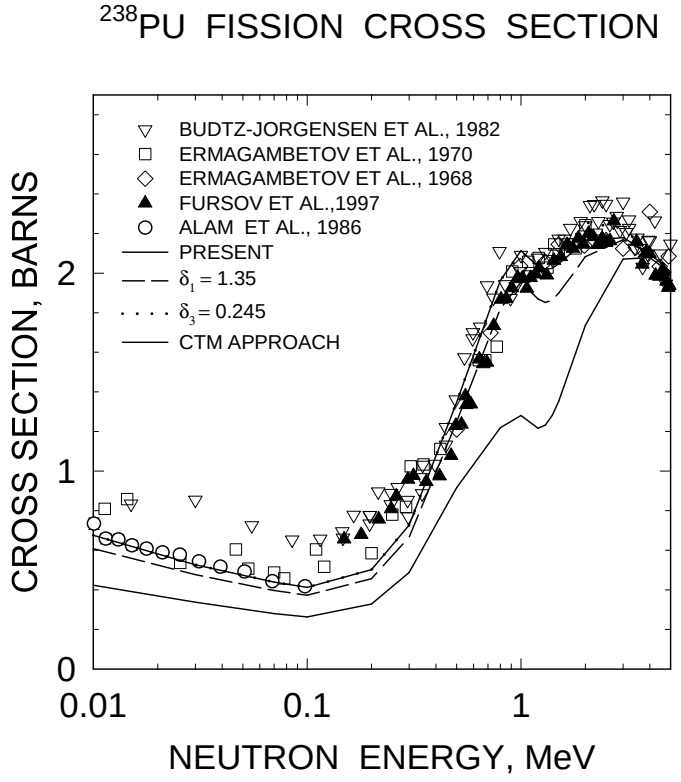
^{238}PU FISSION CROSS SECTION
BUDTZ-JORGENSEN ET AL., 1982
ERMAGAMBETOV ET AL., 1970
ERMAGAMBETOV ET AL., 1968
FURSOV ET AL.,1997
ALAM ET AL., 1986
PRESENT
δ_1 = 1.35
δ_3 = 0.245
CTM APPROACH
CROSS SECTION, BARNS
0
1
2
0.01
0.1
1
NEUTRON ENERGY, MeV

FIG. 1

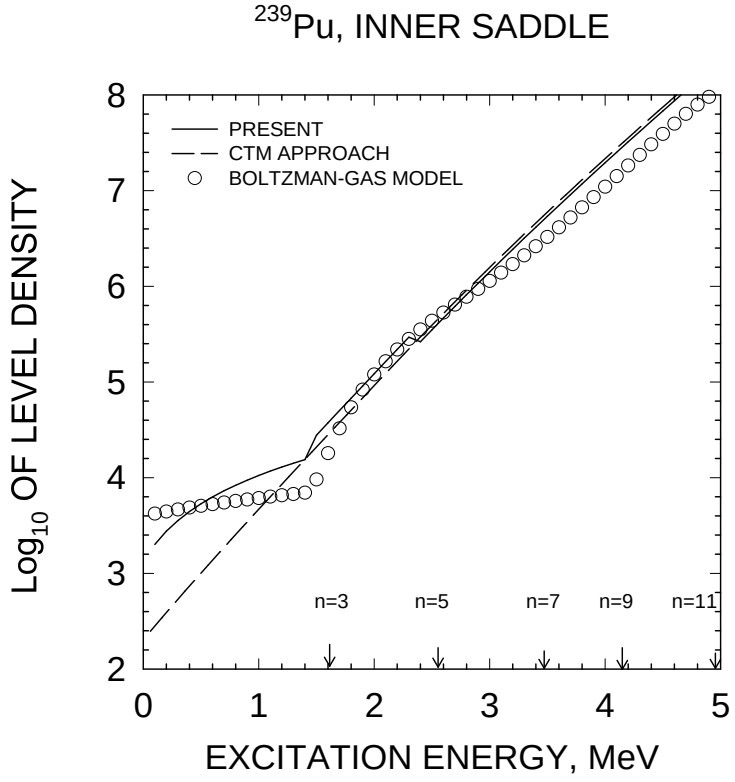
^{239}Pu, INNER SADDLE
PRESENT
CTM APPROACH
BOLTZMAN-GAS MODEL
n=3
n=5
n=7
n=9
n=11
Log$_{10}$ OF LEVEL DENSITY
EXCITATION ENERGY, MeV
0
1
2
3
4
5
2
3
4
5
6
7
8

FIG. 2

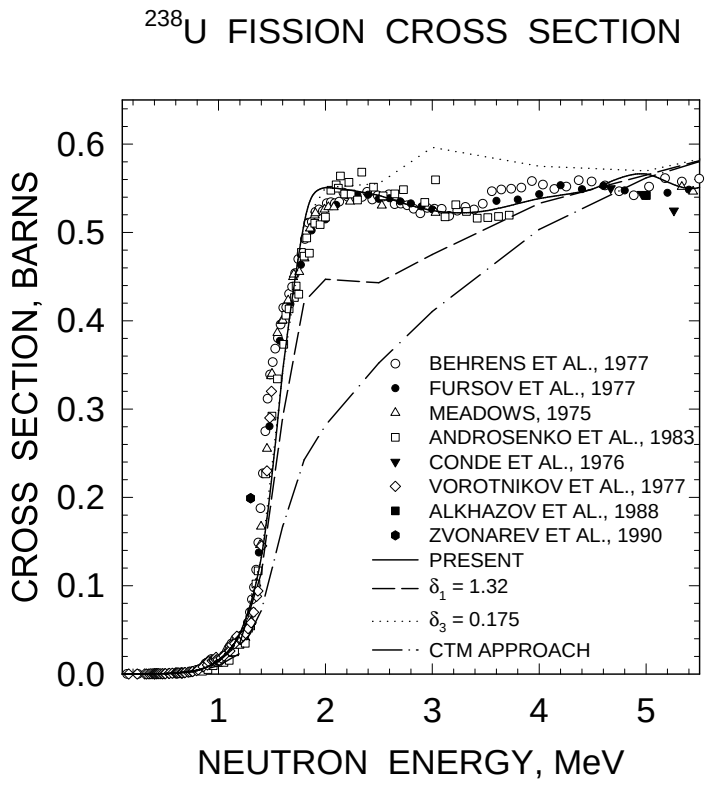
^{238}U FISSION CROSS SECTION
CROSS SECTION, BARNS
NEUTRON ENERGY, MeV
0.0
0.1
0.2
0.3
0.4
0.5
0.6
1
2
3
4
5
BEHRENS ET AL., 1977
FURSOV ET AL., 1977
MEADOWS, 1975
ANDROSENKO ET AL., 1983
CONDE ET AL., 1976
VOROTNIKOV ET AL., 1977
ALKHAZOV ET AL., 1988
ZVONAREV ET AL., 1990
PRESENT
δ_1 = 1.32
δ_3 = 0.175
CTM APPROACH

FIG. 3

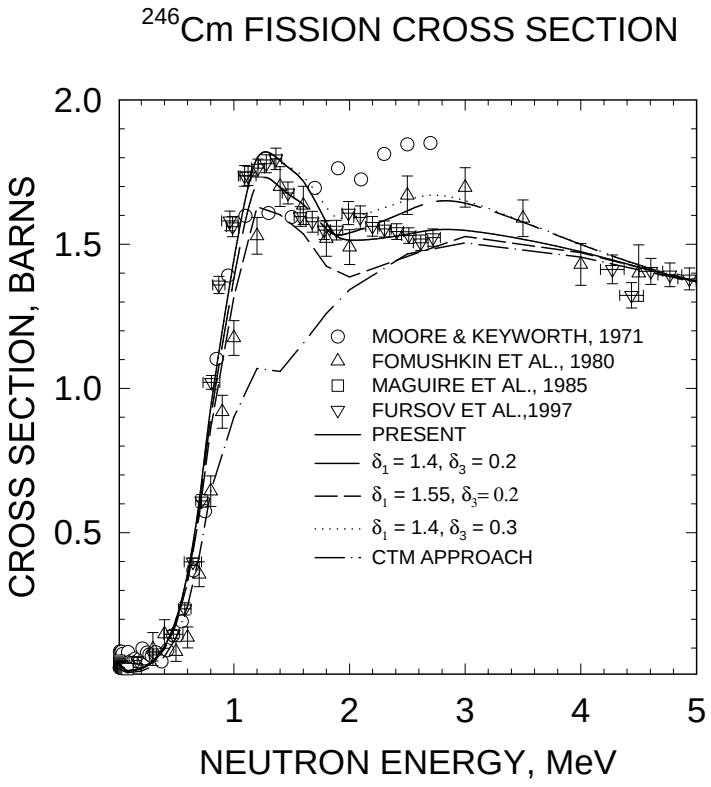
^{246}Cm FISSION CROSS SECTION
CROSS SECTION, BARNS
NEUTRON ENERGY, MeV
2.0
1.5
1.0
0.5
1
2
3
4
5
MOORE & KEYWORTH, 1971
FOMUSHKIN ET AL., 1980
MAGUIRE ET AL., 1985
FURSOV ET AL.,1997
PRESENT
δ_1 = 1.4, δ_3 = 0.2
δ_1 = 1.55, δ_3= 0.2
δ_1 = 1.4, δ_3 = 0.3
CTM APPROACH

FIG. 4

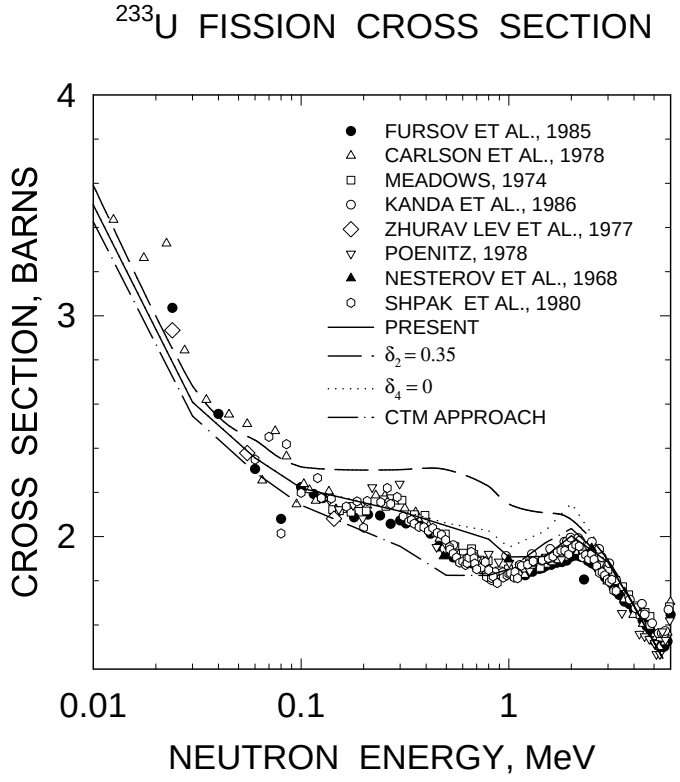
^{233}U FISSION CROSS SECTION
CROSS SECTION, BARNS
NEUTRON ENERGY, MeV
4
3
2
0.01
0.1
1
FURSOV ET AL., 1985
CARLSON ET AL., 1978
MEADOWS, 1974
KANDA ET AL., 1986
ZHURAV LEV ET AL., 1977
POENITZ, 1978
NESTEROV ET AL., 1968
SHPAK ET AL., 1980
PRESENT
$\delta_2 = 0.35$
$\delta_4 = 0$
CTM APPROACH

FIG. 5

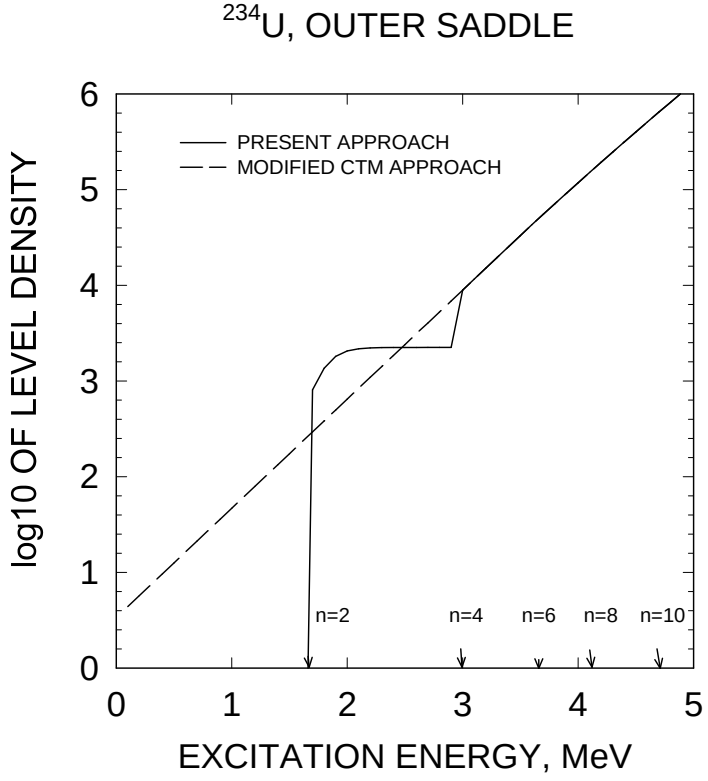
^{234}U, OUTER SADDLE
PRESENT APPROACH
MODIFIED CTM APPROACH
log10 OF LEVEL DENSITY
EXCITATION ENERGY, MeV
n=2
n=4
n=6
n=8
n=10
0
1
2
3
4
5
6

FIG. 6

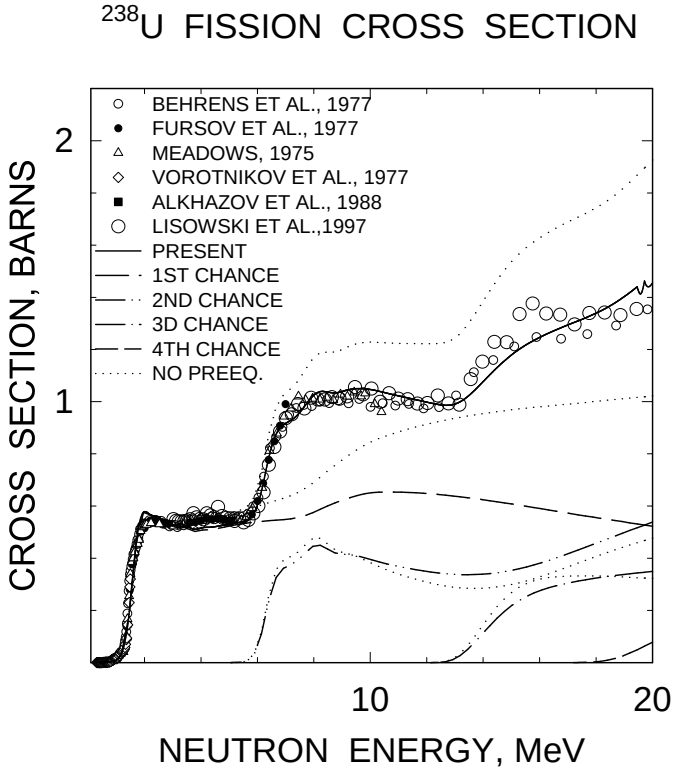
^{238}U FISSION CROSS SECTION
BEHRENS ET AL., 1977
FURSOV ET AL., 1977
MEADOWS, 1975
VOROTNIKOV ET AL., 1977
ALKHAZOV ET AL., 1988
LISOWSKI ET AL.,1997
PRESENT
1ST CHANCE
2ND CHANCE
3D CHANCE
4TH CHANCE
NO PREEQ.
CROSS SECTION, BARNS
2
1
10
20
NEUTRON ENERGY, MeV

FIG. 7

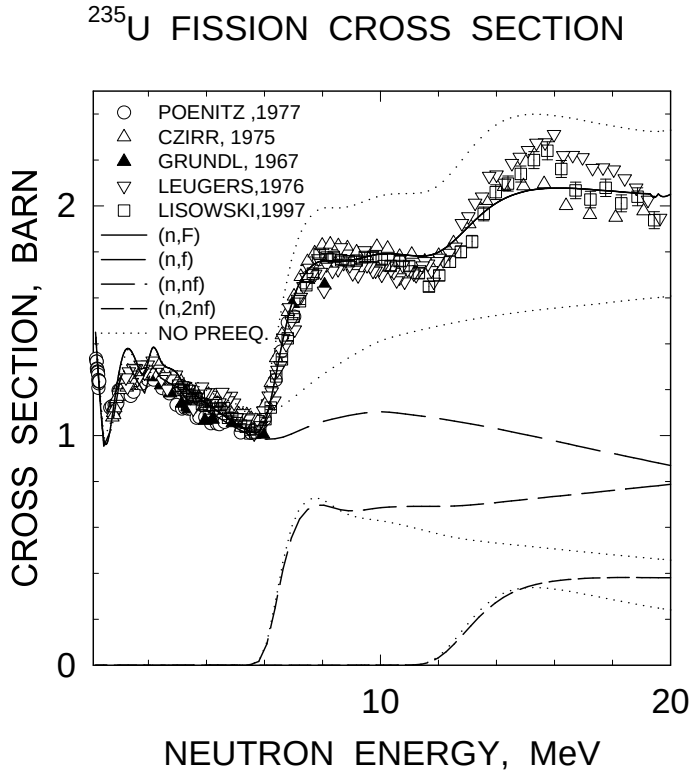
^{235}U FISSION CROSS SECTION
POENITZ ,1977
CZIRR, 1975
GRUNDL, 1967
LEUGERS,1976
LISOWSKI,1997
(n,F)
(n,f)
(n,nf)
(n,2nf)
NO PREEQ.
CROSS SECTION, BARN
0
1
2
10
20
NEUTRON ENERGY, MeV

FIG. 8

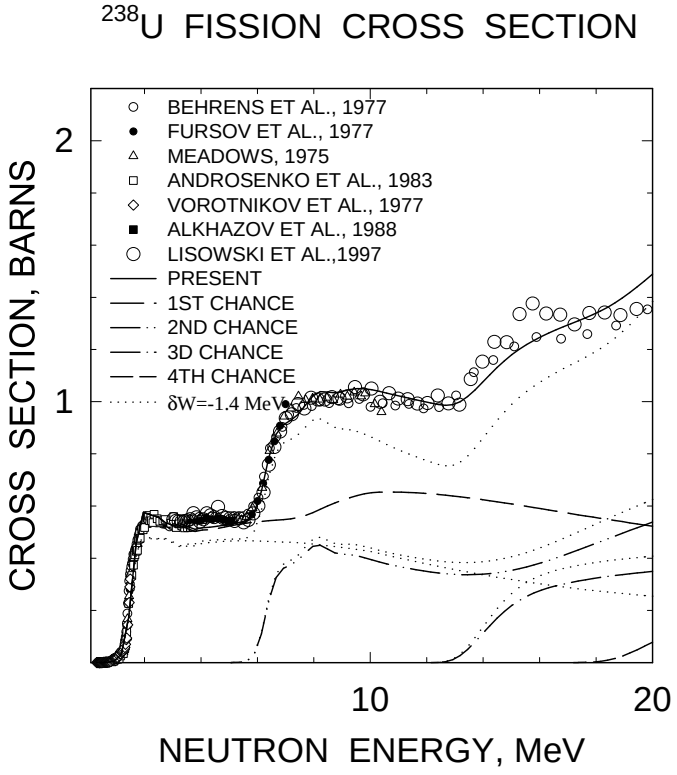
238U FISSION CROSS SECTION
BEHRENS ET AL., 1977
FURSOV ET AL., 1977
MEADOWS, 1975
ANDROSENKO ET AL., 1983
VOROTNIKOV ET AL., 1977
ALKHAZOV ET AL., 1988
LISOWSKI ET AL.,1997
PRESENT
1ST CHANCE
2ND CHANCE
3D CHANCE
4TH CHANCE
δW=-1.4 MeV
CROSS SECTION, BARNS
2
1
10
20
NEUTRON ENERGY, MeV

FIG. 9

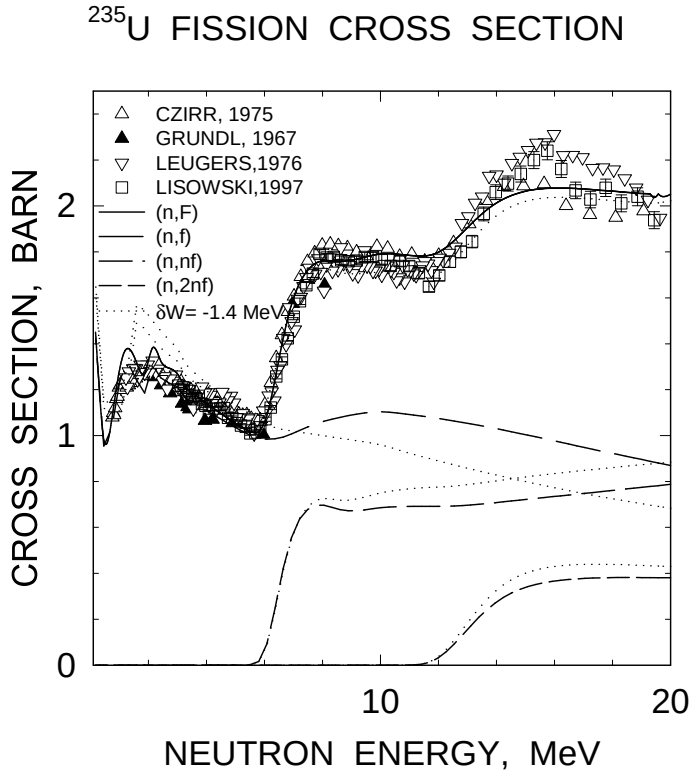
^{235}U FISSION CROSS SECTION
CZIRR, 1975
GRUNDL, 1967
LEUGERS,1976
LISOWSKI,1997
(n,F)
(n,f)
(n,nf)
(n,2nf)
δW= -1.4 MeV
CROSS SECTION, BARN
0
1
2
10
20
NEUTRON ENERGY, MeV

FIG. 10

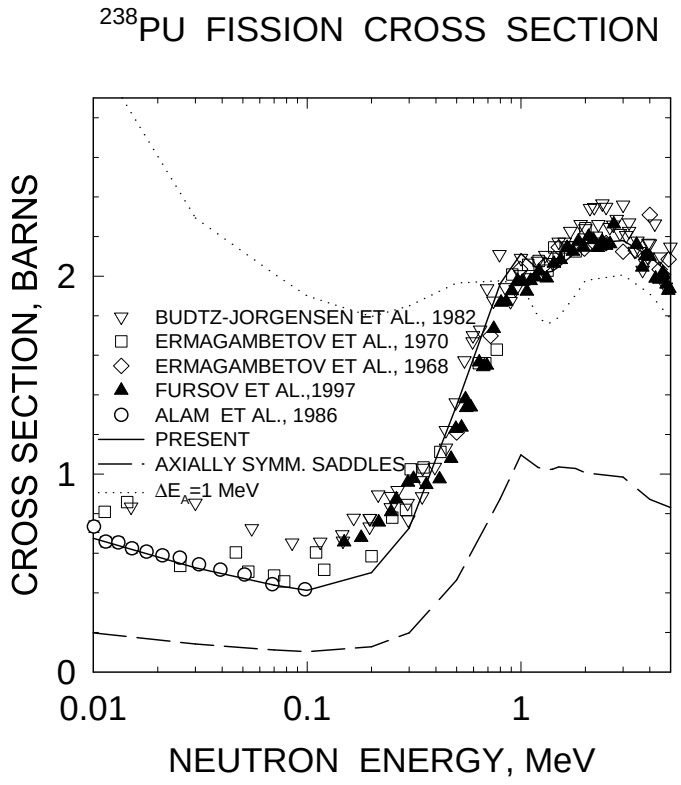
238PU FISSION CROSS SECTION
CROSS SECTION, BARNS
0
1
2
0.01
0.1
1
NEUTRON ENERGY, MeV
BUDTZ-JORGENSEN ET AL., 1982
ERMAGAMBETOV ET AL., 1970
ERMAGAMBETOV ET AL., 1968
FURSOV ET AL.,1997
ALAM ET AL., 1986
PRESENT
AXIALLY SYMM. SADDLES
ΔE_A=1 MeV

FIG. 11

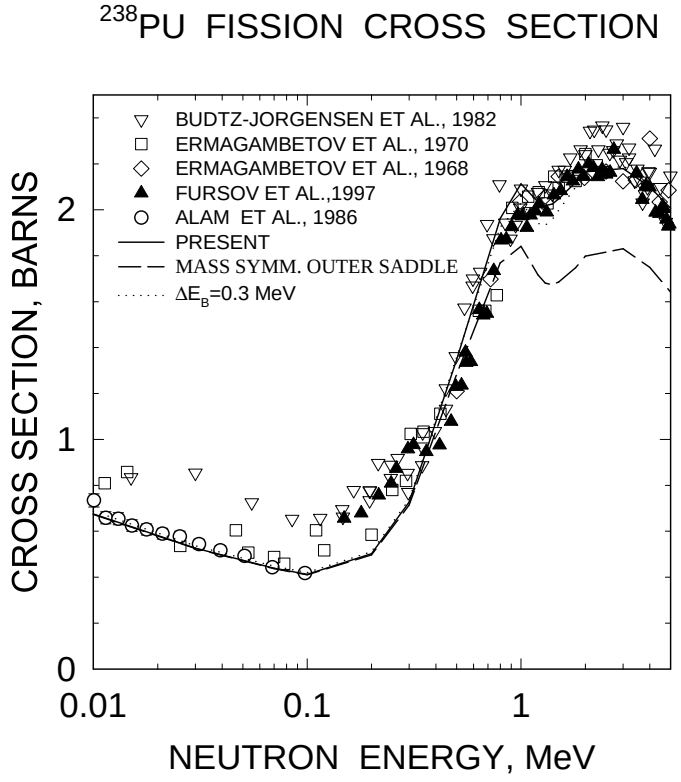
^{238}PU FISSION CROSS SECTION
BUDTZ-JORGENSEN ET AL., 1982
ERMAGAMBETOV ET AL., 1970
ERMAGAMBETOV ET AL., 1968
FURSOV ET AL.,1997
ALAM ET AL., 1986
PRESENT
MASS SYMM. OUTER SADDLE
ΔE$_B$=0.3 MeV
CROSS SECTION, BARNS
0
1
2
0.01
0.1
1
NEUTRON ENERGY, MeV

FIG. 12

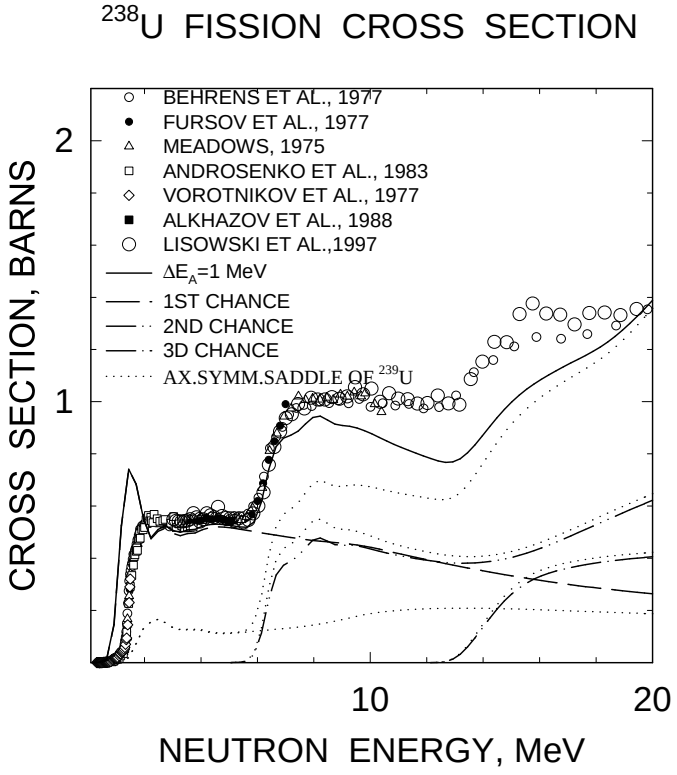
238U FISSION CROSS SECTION
BEHRENS ET AL., 1977
FURSOV ET AL., 1977
MEADOWS, 1975
ANDROSENKO ET AL., 1983
VOROTNIKOV ET AL., 1977
ALKHAZOV ET AL., 1988
LISOWSKI ET AL.,1997
ΔE_A=1 MeV
1ST CHANCE
2ND CHANCE
3D CHANCE
AX.SYMM.SADDLE OF 239U
CROSS SECTION, BARNS
2
1
10
20
NEUTRON ENERGY, MeV

FIG. 13